Competition and Coadsorption of Di-acids and Carboxylic Acid Solvents on HOPG

Feng Tao, Julie Goswami, and Steven L. Bernasek*

Department of Chemistry, Princeton University, Princeton, New Jersey 08544

Received: June 22, 2006; In Final Form: August 9, 2006

The self-assemblies of di-acids HOOC−$(CH_2)_n$−COOH (n = 20, 18, 16, 14, 12, 10) in three solvents hexanoic acid, octanoic acid, and decanoic acid on highly oriented pyrolytic graphite (HOPG) were studied with scanning tunneling microscopy (STM). In the solvent hexanoic acid, solvent molecules coadsorb with HOOC−$(CH_2)_n$−COOH (n = 20, 18, 16) via formation of hydrogen bonds. The solvent octanoic acid coadsorbs with HOOC−$(CH_2)_n$−COOH (n = 20, 18). Decanoic acid only coadsorbs with HOOC−$(CH_2)_{20}$−COOH. In each solvent, the trend of coadsorption between solvent molecules and di-acid molecules decreases with decreasing chain-length of di-acid molecules. These systematic investigations suggest that coadsorption of solvent molecules with di-acid solute molecules is mainly dependent on the relative hydrogen-bond densities in the formed monolayer. This is consistent with the maximization of adsorption heat of the self-assembled monolayers of di-acids dissolved in solvents of carboxylic acids.

1. Introduction

Self-assembly is one of the important approaches to material synthesis. For two-dimensional self-assembly, solvent molecules play an important factor in the formation of molecular self-assembled monolayers at the solid−liquid interface. One basic role of the solvent is the dissolution of solid solutes to form the solutions for molecular self-assembly on solid surfaces, or for further mixing with other solutions for final self-assembly.

Notably, some solvent molecules may self-assemble as well on the solid surface. For these solvent molecules, there is a competition for self-assembly with the solute molecules. They also may form associated self-assembled structures with the solute molecules in terms of coadsorption with the solute on the solid surface. To demonstrate the competition and association of solvent and solute molecules during self-assembly at the solid−liquid interface, a series of di-acid solutes and *n*-carboxylic acid solvents were chosen as a model for study. Because both solute and solvent molecules have carboxylic acid groups, it is expected that they may compete and associate with each other via the formation of hydrogen bonds during self-assembly. To understand the driving force for this competition and association, a series of di-acids HOOC−$(CH_2)_n$−COOH (n = 20, 18, 16, 14, 12, 10) (*C22*, *C20*, *C18*, *C16*, *C14*, and *C12* here represent di-acid solute molecules) with a continual change of hydrogen-bond density, and *n*-carboxylic acids CH_3-$(CH_2)_n$COOH (n = 4, 6, 8) (C6, C8, C10 here represent single-acid solvent molecules) were selected as solutes and solvents, respectively.

STM is the main technique for characterizing the surface structures of the self-assembled monolayers formed. Our studies show that the relative hydrogen-bond density in the structures controls the possibility of coadsorption.

2. Experimental Section

All of the studies described here were performed with a laboratory-built STM operating at the liquid−solid interface under ambient conditions. The single-tube scanner and tip were horizontally mounted and used for scanning. The tip was fabricated by mechanically cutting 0.25 mm platinum/iridium wire (Pt/Ir = 90/10) purchased from Goodfellow. HOPG of ZYA grade was obtained from Advanced Ceramics Corporation. Hexanoic acid (≥99.5%), octanoic acid (99.0%) and decanoic acid (99.5%), docosanedioic acid (≥95.0%), hexadecanedioic acid (≥98.0%), tetradecanedioic acid (≥98.0%), dodecanedioic acid (99.0%) from Aldrich, and octadecanedioic acid (≥95%) and eicosanedioic acid (95%) from TCI America were used without further purification. For the convenience of description, here C6, C8, and C10 represents hexanoic acid, octanoic acid,

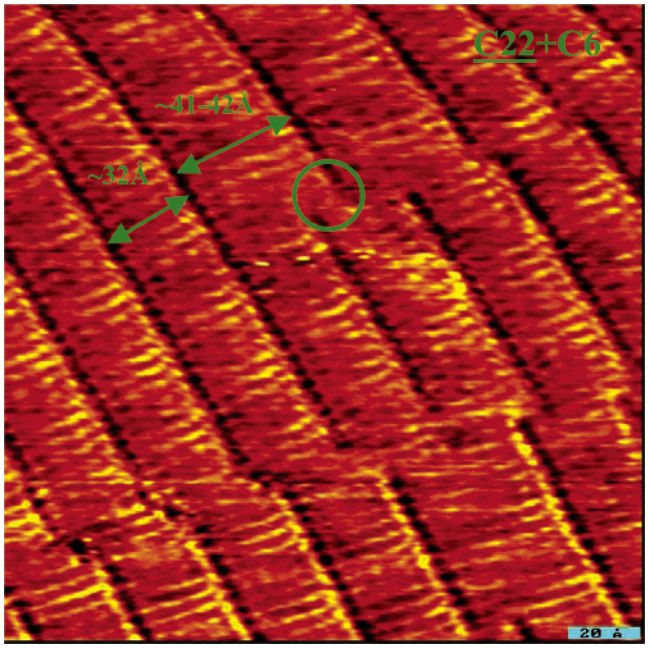

Figure 1. One domain of the *C22*/C6 system. This domain shows the coadsorption between *C22* and C6 lamellae. 183 × 183 Å. V_t = 0.71 V; I_t = 0.77 nA. The green circle shows a sudden switch from coadsorption lamellae into lamella without coadsorption.

* Corresponding author phone: 609-258-4986; fax: 609-258-1593; e-mail: sberna@princeton.edu.

10.1021/jp063923a CCC: $33.50
Published on Web 09/07/2006

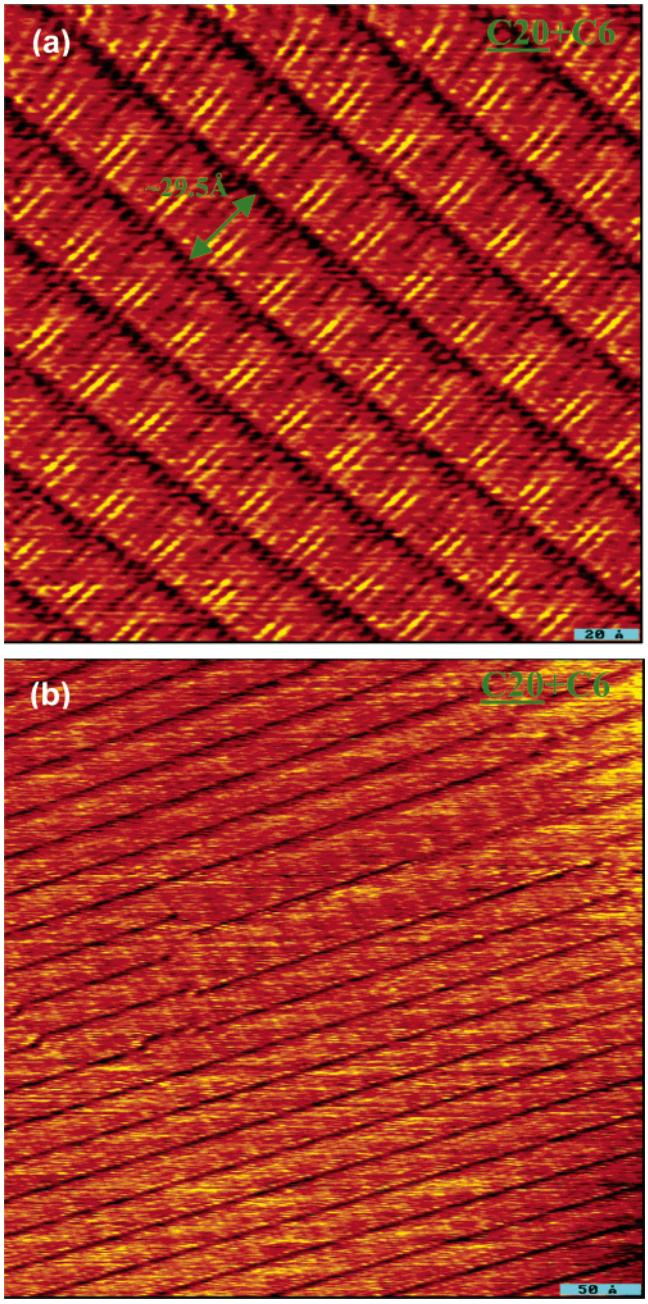

Figure 2. (a) One domain of the *C20*/C6 system (without coadsorption). 202 × 203 Å. $V_t = 0.71$ V; $I_t = 0.66$ nA. (b) One domain of the *C20*/C6 system. This domain shows the coadsorption between *C20* and C6. 400 × 400 Å. $V_t = 0.71$ V; $I_t = 0.66$ nA.

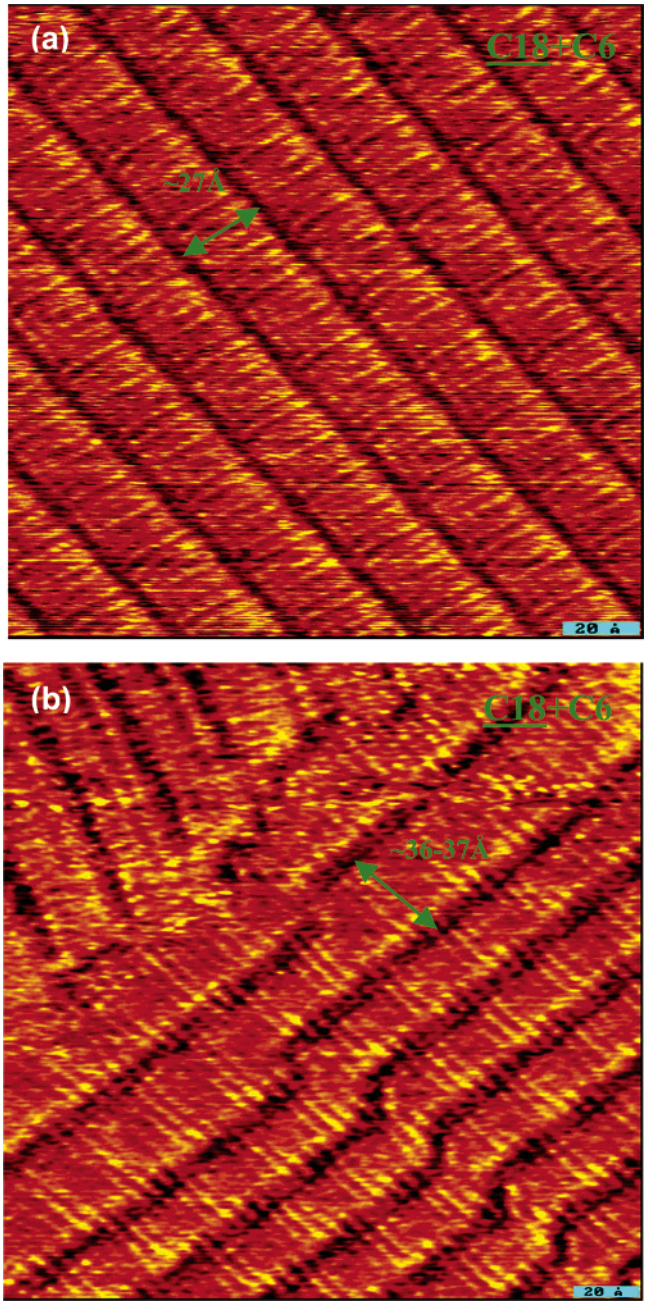

Figure 3. (a) One domain of the *C18*/C6 system (without coadsorption). 170 × 170 Å. $V_t = 0.71$ V; $I_t = 0.65$ nA. (b) One domain of the *C18*/C6 system. This domain shows the coadsorption between *C18* and C6. 200 × 200 Å. $V_t = 0.71$ V; $I_t = 0.65$ nA.

and decanoic acid, respectively, and *C12*, *C14*, *C16*, *C18*, *C20*, and *C22* represent the di-acids.

All solutions were prepared by dissolving solid di-acid into an acid solvent with a concentration of 5 mmol/L (mM). Two other sets of solutions with a concentration of 10 mM and 15 mM were also prepared for examination. The HOPG surface was freshly prepared by cleaving the graphite crystal to expose a mirrorlike surface before imaging. The quality and longevity of a freshly cleaved sample depends somewhat on the ambient humidity conditions, with drier conditions leading to longer lasting substrates. Solutions did not appear to be affected by ambient humidity. Samples were prepared by gently depositing one drop of the prepared solutions (3−5 μL) onto the HOPG surface. Samples were positively biased. All images were collected in a constant current mode.

3. Results and Discussion

Figure 1 is a representative image of *C22* dissolved in C6 (*C22*/C6). The concentration of this solution is 10 mM. Clearly, there are two kinds of lamellae in the self-assembled monolayer. Within the lamellae, the individual molecules pack side-by-side with the carbon backbone of the molecule parallel to the graphite surface, as has been previously seen for long-chain hydrocarbons adsorbed on graphite. Both lamellae have a chain-trough angle of ~90°. However, their widths are different. The narrow one has a width of ~32.0 Å, exactly corresponding to the length of one *C22* di-acid molecule. The width of the wide lamella, ~41.0−42.0 Å is consistent with the total length of one *C22* di-acid and one solvent molecule C6, suggesting a coadsorption of solute *C22* and solvent C6 molecules. This coadsorption is at the level of lamella. Moreover, the coadsorption domains are

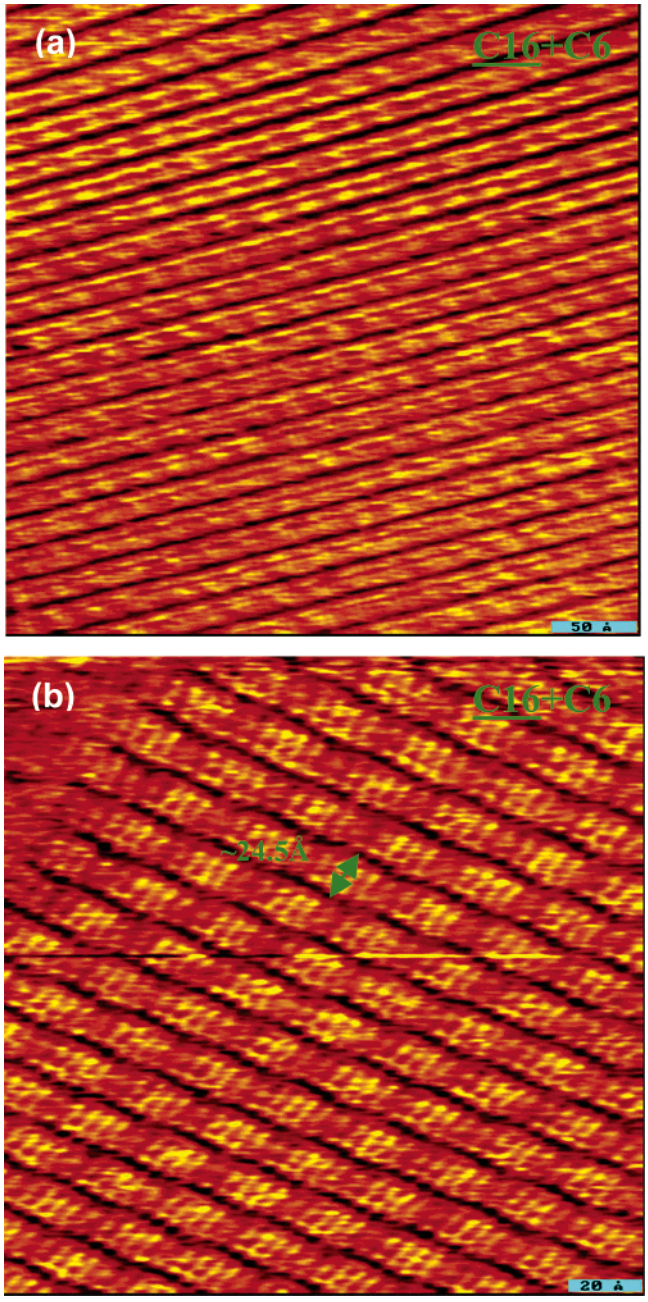

Figure 4. (a) One domain of the *C16*/C6 system (without coadsorption). 200 × 200 Å. $V_t = 1.21$ V; $I_t = 0.75$ nA. (b) Another domain of the *C16*/C6 system (without coadsorption). 380 × 380Å. $V_t = 1.22$ V; $I_t = 0.75$ nA.

not evenly distributed. The propagation of coadsorbed lamella even stops suddenly as marked with the green circle in Figure 1. Note that no regions of lamellae are observed corresponding to C6 adsorbed by itself. The pure solvent acid does not form ordered self-assembled monolayers.

Figure 2 shows two representative images of *C20* di-acid dissolved in C6 with a concentration of 10 mM. There is only one category of lamella in Figure 2a. Each lamella has a width of ~29.5 Å, the molecular length of the *C20* di-acid. In this image, no coadsorption is observed. Other images such as in Figure 2b were observed in the same self-assembled monolayer. In this type of image, coadsorption domains with a width of 38.5−39.5 Å (one *C20* di-acid and one C6 solvent molecule) is observed, though the area of the image of coadsorption lamellae is much lower than that in the image of the *C22*/C6 system. A rough estimate based on the collected images suggests

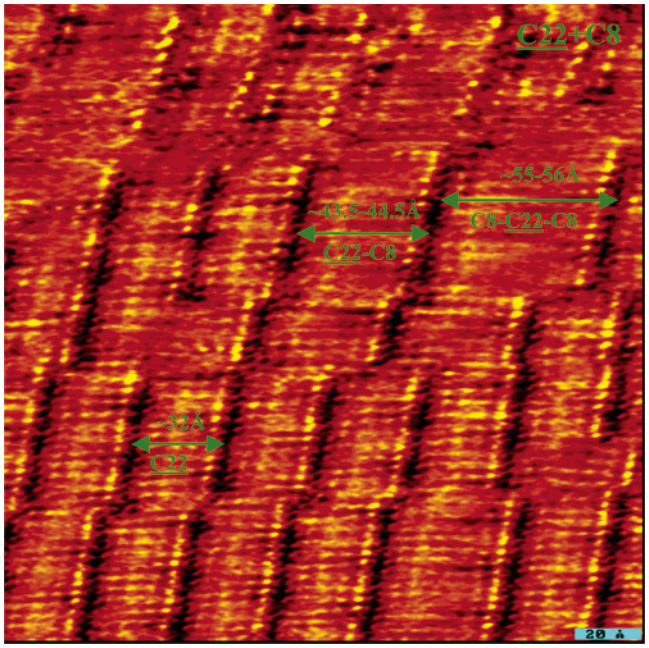

Figure 5. One domain of the *C22*/C8 system. This domain shows the coadsorption between *C22* and C8 lamellae. 200 × 200 Å. $V_t = 0.74$ V; $I_t = 0.87$ nA.

that the molar ratio of solvent (C6) in the self-assembled monolayer is ~8−14%. Notably, this ratio is not the ratio of any individual image. It is the average ratio of several collected images. This ratio is lower than that seen for the *C22*/C6 system. This implies a trend of reduced coadsortion of di-acid and C6 solvent with decreasing chain-length of the di-acid solute.

Figure 3a is a typical image of the *C18*/C6 system. No coadsorption lamella is observed in this image. Figure 3b is an image containing coadsorption lamellae. Among the more than 20 images for this sample, only one-third of the images have coadsorption lamellae. The overall ratio of C6 coadsorption in these examined domains is ~4−10%. The comparison with the *C20*/C6 and *C18*/C6 systems further supports the trend of reduced coadsorption between di-acid and C6 with the decrease of chain length of the di-acid molecule, based on the area of coadsorption lamellae roughly estimated on the basis of the collected images.

Figure 4 shows two typical images of *C16*/C6 solution with different dimensions. Notably, no coadsorption lamellae are observed in these collected images for this system, suggesting no coadsorption in the *C16*/C6 system. The self-assembly of *C14*/C6 and *C12*/C6 systems were also investigated. No coadsorption was found for these solutions, only well ordered lamellae with the di-acid width.

On the basis of these experimental observations for a series of self-assembled systems of (HOOC−$(CH_2)_n$−COOH dissolved in $CH_3(CH_2)_4COOH$), the likehood of coadsorption increases with the increasing chain-length of the di-acid solute. Molecular chain length of these alkanoic acids determines the hydrogen-bond density of a structure formed on HOPG. This trend implies that the relative densities of hydrogen bond of solvent and solute molecules play an important role in controlling coadsorption. To further clarify this trend, the self-assembly of di-acids in other solvents with different chain lengths was studied as well.

For the self-assembled monolayer of *C22* di-acid dissolved in octanoic acid (C22/C8), the coadsorption lamellae are observed in almost all collected images. Figure 5 is one typical image of the *C22*/C8 monolayer. Coadsorption between *C22* and C8 can be clearly identified. Interestingly, there are two

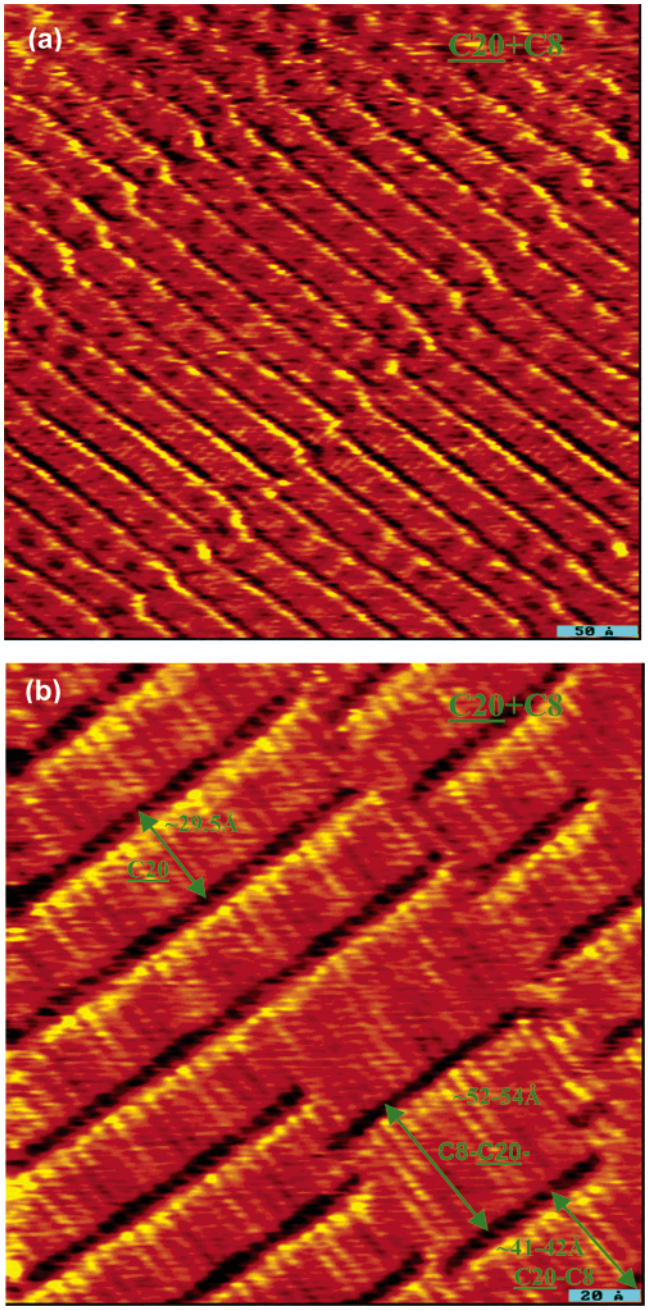

Figure 6. (a) One domain of the *C20*/C8 system (without coadsorption). 400 × 400 Å. $V_t = 0.70$ V; $I_t = 0.72$ nA. (b) One domain of the *C20*/C8 system. This domain shows the coadsorption between *C20* and C8. 180 × 180 Å. $V_t = 0.70$ V; $I_t = 0.72$ nA.

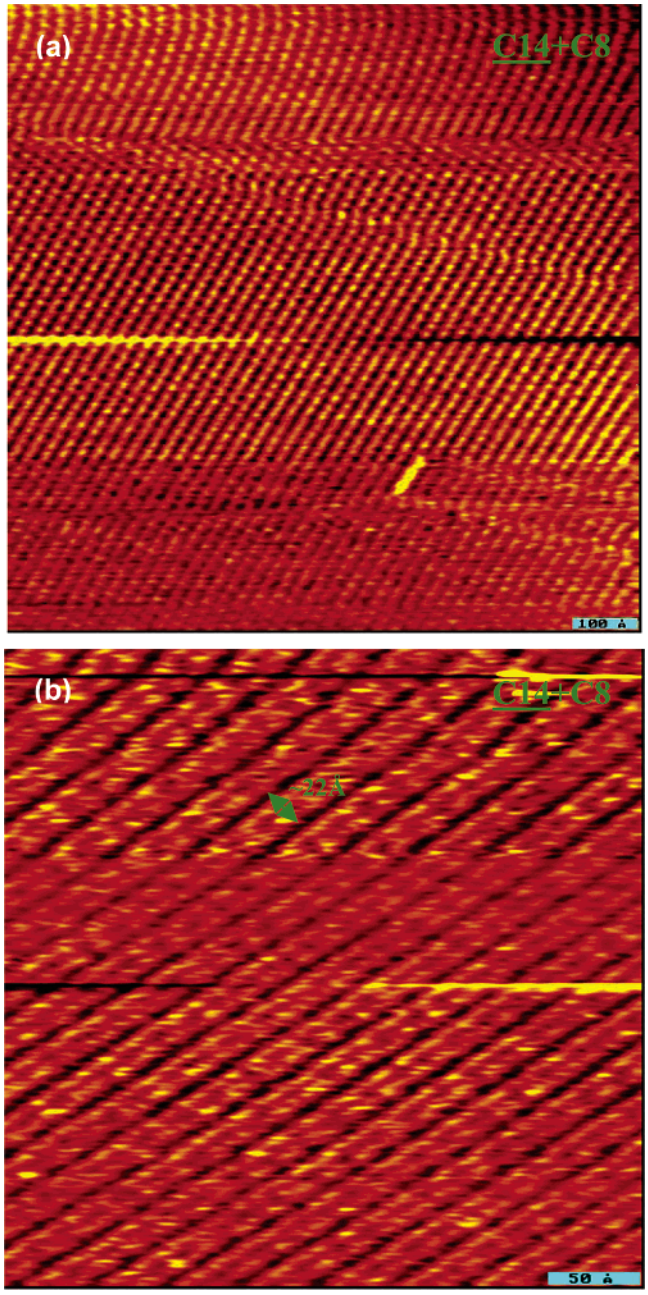

Figure 7. (a) One domain of the *C14*/C8 system (without coadsorption). 1000 × 1000 Å. $V_t = 0.71$ V; $I_t = 0.78$ nA. (b) One domain of the *C14*/C8 system (without coadsorption). 350 × 350 Å. $V_t = 0.70$ V; $I_t = 0.79$ nA.

kinds of coadsorption lamellae marked with *C22*−C8 and C8−*C22*−C8. The molar ratio of solvent C8 in this representative image is ∼20−30%, demonstrating a strong trend for coadsorption between *C22* and solvent C8 molecules. Again, note that no lamellae are observed to form from C8 solvent molecules by themselves.

Two classes of images were observed from the self-assembled monolayer of the *C20*/C8 solution. Figure 6a shows one type of image observed in this system. No coadsorption was observed in this category of image. However, coadsorption was revealed in some images though the overall coadsorption area for this kind of image is not higher than 15%. Figure 6b is an example of this sort of image, in which two coadsorption lamellae labeled with *C20*−C8 and C8−*C20*−C8 were observed.

However, no coadsorption domains were found in all the images collected in the self-assembled monolayer of *C18*/C8 solution, indicating no solvent−solute coadsorption in this system. The evolution of coadsorption from *C22*/C8, *C20*/C8 to *C18*/C8 implies a decreasing likehood of coadsorption with decreasing chain length of the di-acid solute, consistent with the reduced trend observed for di-acids/C6 systems. Examination of the self-assembled monolayer from solutions of *C16*/C8, *C14*/C8, and *C12*/C8 show no coadsorption lamellae. Figure 7 shows two typical images observed from the self-assembled monolayer of the *C14*/C8 system for example.

Coadsorption occurs with the *C18*/C6 solution, but not the *C18*/C8 solution. This difference suggests that the chain-length of the solvent molecules also plays an important role in the coadsorption. To further understand the chain-length effect of solvent molecules on the coadsorption trend, C10 was used as a solvent for studies of self-assembly of di-acids in carboxylic acid solvent.

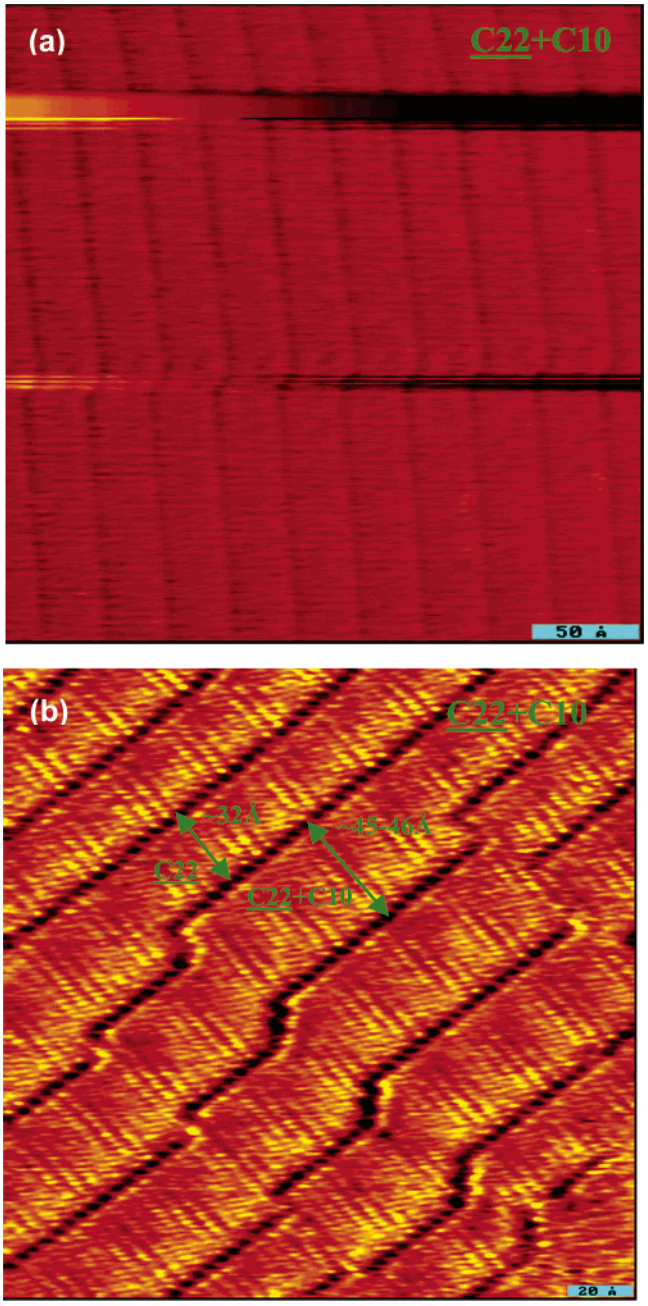

Figure 8. (a) One domain of the *C22*/C10 system (without coadsorption). 302 × 302 Å. $V_t = 0.70$ V; $I_t = 0.73$ nA. (b) One domain of the *C22*/C10 system. This domain shows the coadsorption between *C22* and C10. 201 × 201 Å. $V_t = 0.70$ V; $I_t = 0.74$ nA.

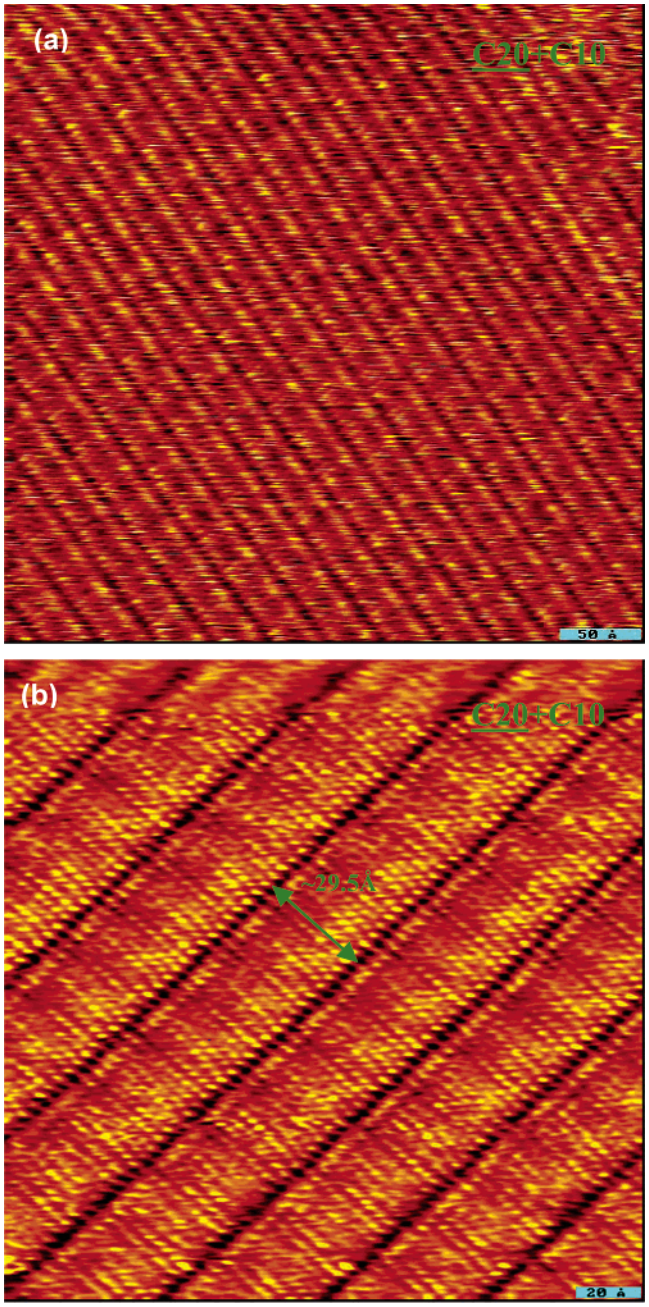

Figure 9. (a) One domain of the *C20*/C10 system (without coadsorption). 402 × 402 Å. $V_t = 0.71$ V; $I_t = 0.76$ nA. (b) One domain of the *C20*/C10 system (without coadsorption). 200 × 200 Å. $V_t = 0.71$ V; $I_t = 0.76$ nA.

Because C10 is a solid under ambient condition, it was used as a solvent after being dissolved in a 1:1 mixture of propanoic acid and phenyloctane. The studied di-acid was dissolved into this solvent with a molar ratio of 1:100 between di-acid and C10 solvent. For the self-assembled monolayer of the *C22*/C10 solution, two categories of images were observed. In the first kind of image such as seen in Figure 8a, all the lamellae are made only from *C22* molecules. Figure 8b is a representative image of another category of domain containing coadsorption lamellae. In this image, some *C22* lamellae coadsorb with C10 molecules. However, no coadsorption was observed for *C20*/C10, *C18*/C10, *C16*/C10, *C14*/C10, or *C12*/C10 systems prepared in this same way. Figure 9 shows two typical images of the *C20*/C10 system, demonstrating the absence of coadsorption of *C20* with C10. Thus, in the di-acid + C10 systems, the trend of coadsorption of di-acid with solvent molecules also decreases with decreasing chain length of the di-acid molecule. According to this trend, it is expected that C24 may coadsorb with C10 on HOPG, though the C24 di-acid is not available commercially, and this expectation was not tested experimentally.

Comparison of these three series of self-assembled systems shows a different point for conversion from noncoadsorption to coadsorption with increasing chain-length of the di-acid solutes. Figure 10 schematically presents this trend for coadsorption for the three series. Definitely, the conversion point is strongly dependent on the chain length of the solvent molecules. The solid spots show that there is coadsorption between two corresponding solute and solvent molecules. The circles show no coadsorption. The dashed line is the boundary between coadsorption systems and no-coadsorption systems.

To rationalize the trend of coadsorption in each series and the evolution of the conversion point in the three series, the

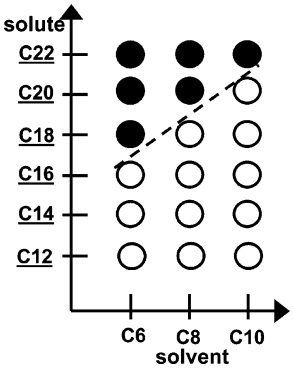

Figure 10. Evolution of the self-assembly of a series of di-acids (*C22*, *C20*, *C18*, *C16*, *C14*, and *C12*) dissolved in different carboxylic acid solvents (C6, C8, and C10). Solid spot shows that solvent molecules can coadsorb with di-acid molecules. Circle shows no coadsorption between solvent and solute.

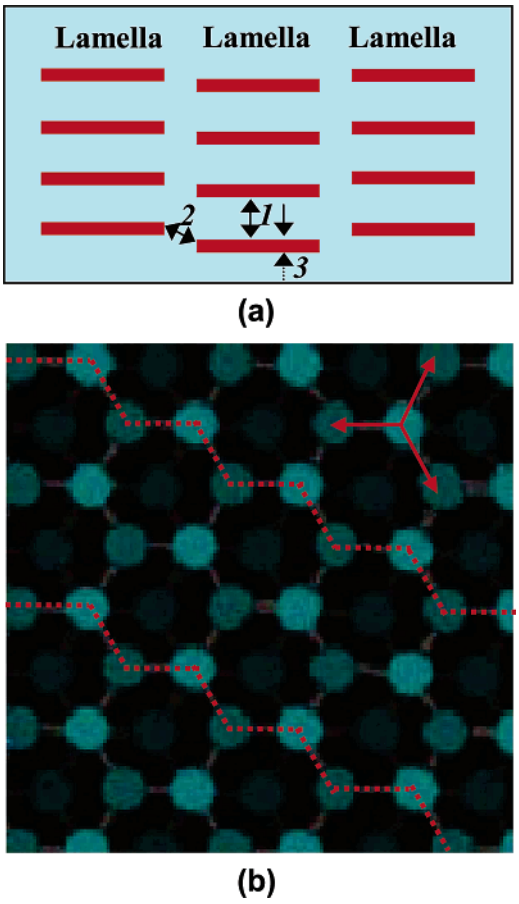

Figure 11. (a) Scheme of intermolecular van der Waals force (1) in a lamella, intermolecular van der Waals interaction and/or hydrogen bonds, (2) between two adjacent lamellae, and van der Waals interaction, (3) between molecules and substrate experienced by each molecule in the self-assembled monolayer. (b) Scheme showing the lattice match between zigzag carbon skeleton of *all-trans* organic molecules and lattice of graphite substrate. Dashed lines represent molecular carbon skeletons.

weak nonconvalent interactions in the self-assembled structure are considered. Each molecule of one self-assembled monolayer experiences three kinds of weak interactions including van der Waals forces between two adjacent molecules in a lamella, van der Waals, and/or hydrogen bond interactions between molecules and the adjacent molecules of the adjacent lamellae, and the van der Waals interactions between molecules and the underlying surface lattice of HOPG. The interaction between the first

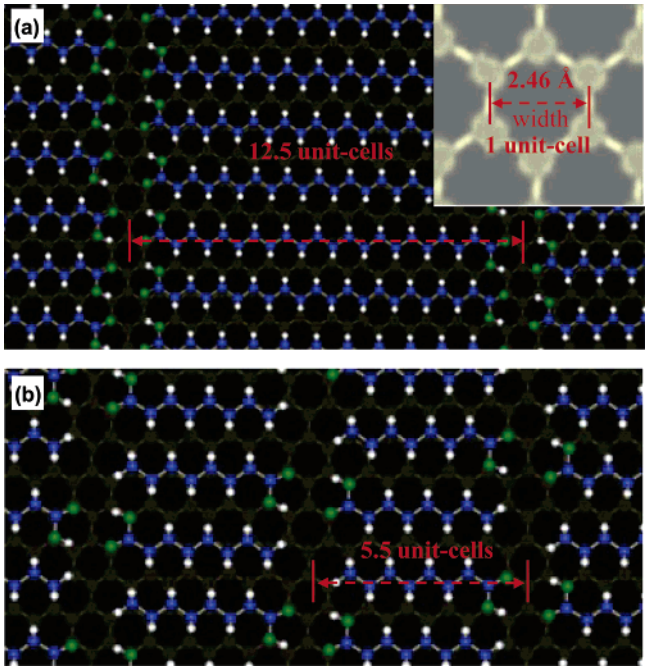

Figure 12. (a) Molecular packing pattern of *C22* on HOPG without coadsorption. This structural model shows the hydrogen-bond density of *C22*. The inset shows the width of one hexagonal unit cell along one zigzag extension direction. (b) Scheme showing the hydrogen-bond density of C8.

monolayer and subsequent layers above it is expected to be much weaker, and more dynamic, as molecules adsorb and redissolve in the solvent above. This interaction is not expected to affect the first monolayer structure significantly, and is not taken into consideration in the analysis here. Figure 11a schematically presents the three weak interactions for one molecule of a self-assembled monolayer on HOPG. Previous studies[1] suggest that one of the major driving forces for forming ordered self-assembled structures of organic molecules from solution, particularly long-chain organic molecules on HOPG, is the steric match between the zigzag lattice of the HOPG surface (with a C−C bond length of 1.42 Å) and the zigzag pattern of the *all-trans* carbon skeleton (with a C−C bond length of 1.46 Å) (Figure 11b), though this issue is controversial.[2,3] This lattice match maximizes the van der Waals interaction between the self-assembled organic molecules and the HOPG substrate.

In the self-assembled structure of di-acids without coadsorption, each lamella is made from di-acid molecules. In Figure 12a, each docosanedioic acid molecule forms four hydrogen bonds with two other di-acid molecules. Thus, the hydrogen-bond density, the number of hydrogen bonds per substrate unit-cell (defined by the inset of Figure 12a) along the chain direction is 2/12.5. Similarly, the hydrogen-bond densities of the self-assembled monolayers of *C20*, *C18*, *C16*, *C14*, and *C12* without coadsorption are 2/11.5, 2/10.5, 2/9.5, 2/8.5, and 2/7.5, respectively. Clearly, the hydrogen-bond density of the di-acid increases with decreasing chain length. The density of hydrogen bonds of C8 (octanoic acid) lamella by itself is 1/5.5 (Figure 12b). By comparison, the hydrogen-bond density of the solvent molecule C8 is larger than that of *C22* and nearly the same as that of *C20*. The hydrogen bond density for octanoic acid lamella is smaller than that of *C18*, *C16*, *C14*, and *C12* di-acids. The relative hydrogen-bond density is in good agreement with the trend of coadsorption of di-acids in solvent C8 shown in Figures 5, 6, 7, and 10. Thus, whether di-acid coadsorbs with one acid solvent or not is determined by the hydrogen-bond density of

the solute molecule adlayer. It is understandable that the coadsorption of *C22* with C8 in terms of the partial replacement of *C22* with solvent C8 molecules increases the overall hydrogen bond density in the structure, and therefore, enhances the stability of the self-assembled monolayer, as it does with C20. However, replacing *C18*, *C16*, *C14*, and *C12* with solvent C8 molecule will definitely lower the overall stability of the self-assembled monolayer. Therefore, no coadsorpiton of C8 molecules was observed in these monolayers.

Compared to the solvent C8 molecule, the C6 solvent molecule has a slightly higher hydrogen-bond density (1/4.5). It can coadsorb with *C22*, *C20*, and *C18* di-acids, as shown in Figures, 1, 2, 3, 4, and 10. However, solvent C10 only coadsorbs with *C22* due to its lower hydrogen-bond density of 1/6.5 (Figures 8, 9, and 10). Thus, the evolution of the crossover points (marked with a dashed line in Figure 10) from coadsorption to noncoadsorption is determined by the hydrogen-bonding density of the formed overlayers. Overall, whether one di-acid molecule coadsorbs with one acid solvent mainly depends on the relative value of the hydrogen-bond density between solute and solvent. If the latter is larger, the coadsorption occurs because the partial replacement of solvent increases the hydrogen-bond density of the self-assembled monolayer. If the former is larger, this kind of coadsorption cannot occur.

The replacement of di-acid molecules with solvent molecules possibly slightly weakens the intermolecular van der Waals forces and molecule-substrate van der Waals interactions due to a slightly lower density of CH_2 units in the coadsorption self-assembled monolayer, due to the shorter chain length of the acid solvent molecule in contrast to the di-acid molecule. The lower density of CH_2 units decreases the stability of the domain to some extent, resulting in a negative effect for coadsorption of solvent molecules with di-acid. This increased energy due to the lower stability resulting from lower density of CH_2 units, is difficult to estimate due to the absence of a measured van der Waals force per CH_2 unit between two adjacent molecules and the adsorption heat per CH_2 unit for these molecules on HOPG. On the other hand, the increased hydrogen-bond density decreases the energy of the coadsorption monolayer. For the self-assembled monolayer from the *C22*/C8 solution, the number of hydrogen bonds is increased by 3m/11 for an area occupied by m *C22* molecules,[4] assuming all the *C22* molecules were to be replaced by C8 solvent molecules. Using the intermolecular hydrogen-bond strength of carboxylic acid in the vapor phase, $E_{hb} = 7.5$ kcal/mol (31.8 kJ/mol),[5,6] the coadsorption enhances the stability of the coadsorption monolayer by $(3m/11)E_{hb}$ (95.4 m/11 kJ/mol). Upon replacement in the coadsorbed layer, the number of CH_2 units is decreased by 3.8m.[7] However, to quantitatively understand the trend of coadsorption reported here, the heat of adsorption of each CH_2 unit for these coadsorption molecules is needed. Some experimental determinations of hydrocarbon adsorption energies on graphite as a function of chain length[1,8] have been made. Similarly, hydrocarbon adsorption on gold has been studied as a function of chain length.[9] For hydrocarbons on graphite, the adsorption energy per methylene unit is estimated as 6.3 kJ/mol.[1,8] For adsorption on gold, it is found to be 6.2 ± 0.2 kJ/mol per methylene unit. These values likely overestimate the change in adsorption energy in these coadsorption systems per methylene unit, since replacement of a solute molecule with a solvent molecule in the overlayer changes the number of CH_2-surface interactions per unit area, as well as the number of CH_2-CH_2 (chain−chain) interactions per unit area. Coadsorption will decrease the chain−chain van der Waals interactions due to the decreased density of CH_2 units upon replacement of *C22* solute molecules with C8 solvent molecules. Notably, if the difference in molecular chain length between di-acid solute and acid solvent is further increased, the decrease in adsorption energy due to the decrease of CH_2 units upon this kind of replacement may play a more important role than the increase of hydrogen bond density in determining whether a coadsorption occurs. Any more quantitative treatment of this effect would need better estimates of the per methylene chain−chain interaction energy.

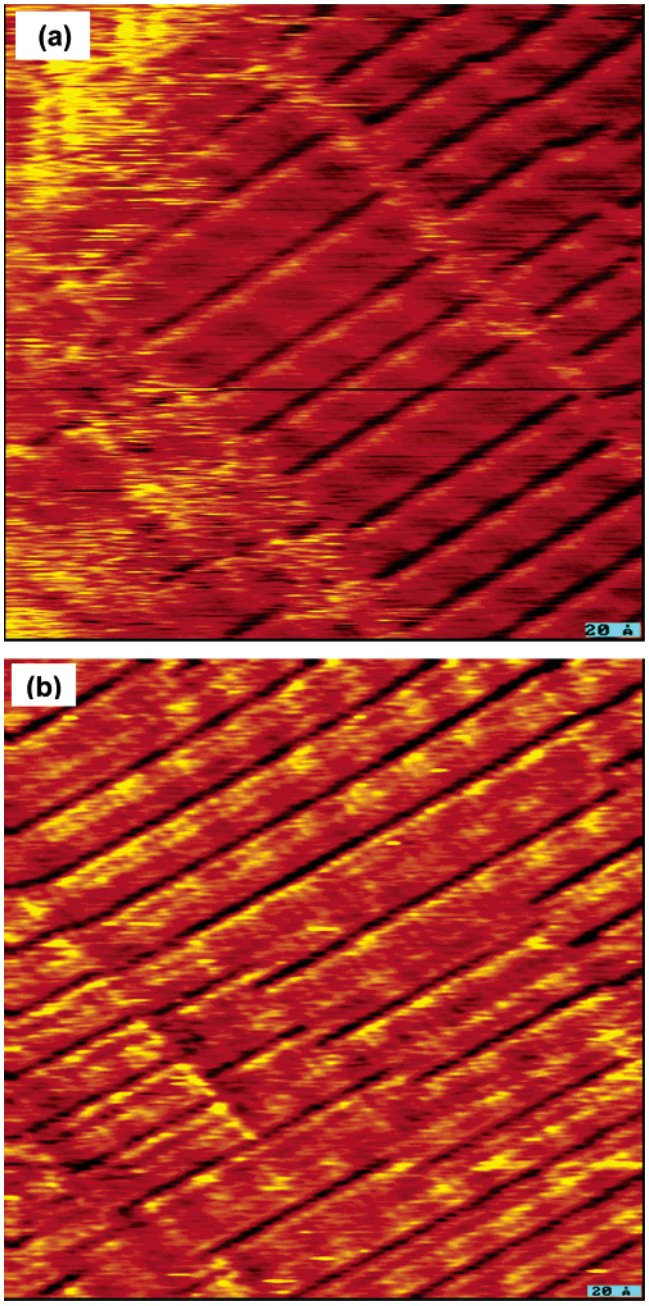

Figure 13. (a) One domain of both *C22* and *C14* with an equal molarity dissolved into C8. 240 × 240 Å. $V_t = 0.70$ V; $I_t = 0.76$ nA. (b) One domain of both *C22* and *C14* with an equal molarity dissolved into C8. 250 × 250 Å. $V_t = 0.88$ V; $I_t = 0.81$ nA.

We suggest that the relative density of hydrogen bonds of di-acid solute and carboxylic acid solvent plays the dominant role in determining whether solvent molecules can coadsorb with the di-acid solute. The importance of hydrogen-bond density in molecular coadsorption was further confirmed in a solution of *C22* and *C14* dissolved in C8. Compared to the self-

assembled monolayer of *C22* dissolved in C8, *C22* does not coadsorb with C8 but does coadsorb with *C14* in a solution of 50% molar *C22* + 50% molar *C14* dissolved in C8. Figure 13 presents two representative coadsorption domains of *C22*/*C14*. As noted, *C14* does not coadsorb with solvent molecule C8, but *C22* does. Thus, the coadsorption between *C22* and C8 competes with coadsorption of *C22* with *C14* in the *C22* + *C14*/C8 system. Because *C14* can form lamellae with a higher hydrogen-bond density than C8, only the *C14* coadsorbs with *C22* as shown in Figure 13.

4. Summary

The self-assembly of di-acids HOOC−$(CH_2)_n$−COOH (n = 20, 18, 16, 14, 12, 10) in three solvents, hexanoic acid, octanoic acid, and decanoic acid, on HOPG was studied with STM. In the hexanoic acid solvent, solvent molecules coadsorb with HOOC−$(CH_2)_n$−COOH (n = 20, 18, 16), forming hydrogen bond stabilized layers. The octanoic acid solvent molecule coadsorb with HOOC−$(CH_2)_n$−COOH (n = 20, 18). Decanoic acid only coadsorbs with HOOC−$(CH_2)_{20}$−COOH. In each solvent, the trend of coadsorption between solvent molecules and di-acid molecules decreases with decreasing chain-length of the di-acid molecules. These systematic investigations suggest that whether solvent molecules can coadsorb with di-acid solute molecules or not, mainly depends on the relative hydrogen-bond densities in the formed layers between di-acid and solvent acid, consistent with the maximization of adsorption heat of the self-assembled monolayers of di-acids dissolved in solvents of carboxylic acids.

Acknowledgment. We acknowledge partial support of this research by the National Science Foundation, CHE-0313801. F.T. acknowledges the support of the Harold W. Dodds Graduate Fellowship of Princeton University.

References and Notes

(1) Groszek, A. J. *Proc. R. Soc. London, Ser A.* **1970**, *314*, 473.

(2) Rabe, J. P.; Buchholz, S. *Science* **1991**, *253*, 424.

(3) Cincotti, S.; Rabe, J. P. *Appl. Phys. Lett.* **1993**, *62*, 3531.

(4) m/11 = 25m/11 × 1 − m × 2. Since each *C22* and C8 molecule occupies 12.5 and 5.5 unit cells, respectively, the area occupied by m *C22* di-acid molecules can be replaced by 25 m/11 C8 solvent molecules.

(5) Vinogradov, S. N.; Linnell, R. H. *Hydrogen Bonding*; Van Nostrand Reinhold Co.: New York, 1971.

(6) The strength of the hydrogen-bond formed between two di-acid molecules and between one di-acid molecule and one solvent acid molecule is not available. Here we take the intermolecular hydrogen-bond strength of propionic acid (7.5 ± 0.6 kcal/mol) as a reference.

(7) 8 m = 22 × m − 8 × 25 m/11. 22 m is the number of CH_2 units when this area only adsorbs *C22* molecules. 8 × 25 m/11 is the number of CH_2 units when this area occupied by *C22* molecules is replaced by C8 solvent molecules.

(8) Kiselev, A. Russ. J. *Phys. Chem.* **1961**, *35*, 111.

(9) Wetterer, S. M.; Lavrich, D. J.; Cummings, T.; Bernasek, S. L.; Scoles, G. *J. Phys. Chem. B* **1998**, *102*, 9266.